Carbon 121 (2017) 106–113

Contents lists available at ScienceDirect

Carbon

journal homepage: www.elsevier.com/locate/carbon

Characterization of nanostructured carbon CMK-3 by means of Monte Carlo simulations

Víctor Yelpo, Valeria Cornette, Juan Pablo Toso, Raúl H. López*

Dpto. de Física. INFAP "Giorgio Zgrablich", CONICET – Universidad Nacional de San Luis, Av. Ej. de los Andes 950, San Luis, Argentina

ARTICLE INFO

Article history:
Received 14 February 2017
Received in revised form
19 May 2017
Accepted 20 May 2017
Available online 24 May 2017

ABSTRACT

A structural model of mesoporous carbon (CMK-3) prepared from the templating of SBA-15 silica materials named *M_CMK3* and a mixed geometry model, representing the porous space as a collection of slit, cylindrical and M_CMK3 pores, is theoretically evaluated, developed and applied to the characterization of an experimental sample [1]. By using the Monte Carlo simulation method (off lattice), families of N_2 adsorption isotherms are generated for cylindrical, slit and M_CMK3 geometries corresponding to different pore sizes. Then, the three geometric families of isotherms (kernels) are used to fit the experimental N_2 adsorption data corresponding to CMK-3 materials, allowing for the determination of the micro and mesopore volume and the corresponding Pore Size Distribution (PSD). The same experimental data were fit using different mixed geometry models, and from the analysis of the effect of different kernels on the resulting PSD, it is concluded that the proposed mixed geometry model can capture in more detailed the textural and energetic features of nanostructured carbon CMK-3. Finally, using a virtual solid and pseudo-experimental adsorption data, the importance of the pore geometry and its effects on the PSD and isosteric enthalpy of adsorption are studied.

1. Introduction

Nanostructured carbons, due to their surface properties and stability, are very attractive for applications in various areas, such as energy storage, water purification, adsorption, catalysis, electrochemistry, and other fields. Ryoo et al. [2] reported the synthesis of a new type of mesoscopically ordered nanoporous (or mesoporous) carbon molecular sieve called as CMK-3 by carbonizing sucrose inside the pores of a SBA-15 mesoporous silica molecular sieve.

Nanostructured carbon materials allow precise control over their textural properties, which is vital for specific applications. The use of ordered mesoporous templates allows obtaining carbons with high specific surface areas (ca. 2000 m^2/g) and pore volumes (ca. 1.5 cm^3/g).

Other techniques (XRD and TEM [3]) are currently used to obtain the pore sizes of previously synthesized CMK-3. However, the nitrogen gas adsorption allows a pore size/textural analysis, which is necessary to fully understand the properties and porous structure of these nanostructured carbons. The usual method to characterize the texture of ordered mesoporous materials (OMM), is the N_2 adsorption-desorption isotherm at 77 K [4–7]. Besides experimental and theoretical works there are many simulation studies that try to improve the study of this class of materials from the adsorption data [8,9]. Furthermore, the main problem in the characterization of nanomaterials is the correct determination of the PSD and the surface area from adsorption isotherms of a probe molecule. The method for the determination of the PSD by means of simulation starts by proposing a model to represent the relevant characteristics of the real material. It is important to stress the fact that such model is a first approximation to mimic the real porous structure, and an idealization meant to reproduce properly the adsorptive properties of the material.

The cylindrical model considers the interstitial space between the nanorods as a collection of independent cylindrical pores with different sizes and is habitually assumed for the characterization of CMK-3-type materials (although, the porous space between these rods have a complex shape [10]) and has been recently used in determining their PSD using the new QSDFT method [1]. In that work the hybrid kernels of the theoretical isotherms were constructed in a restrictive manner, where the slit kernel was only used for the micropore region while the cylindrical one for the mesoporous region. More recently, Barrera et al. [11] obtained similar PSD by using Gran Canonical Monte Carlo simulation (GCMC) and

* Corresponding author.
E-mail addresses: rlopez@unsl.edu.ar, lalolopez@gmail.com (R.H. López).

http://dx.doi.org/10.1016/j.carbon.2017.05.085
0008-6223/

an unique kernel composed by the isotherms obtained for both slit and cylindrical geometries for all pores range, showing that the exclusive contribution of the slit pores in the micropore region was in agreement with the mentioned above and with the experimental evidence that indicates that the micropores are located within the carbon rods of the of CMK-3 materials [12].

As discussed above, several authors (using simple geometries such as spheres, cylinders, etc.) [1,13] have proposed a mixed model in such a way that the pore size distribution can be obtained over the complete micro and mesopore range. Although it is possible to conclude that the CMK-3 texture can be modeled with cylindrical geometry for primary mesopores and slit geometries for micropores, it is our intention to discuss the necessity of improving the structural model for this kind of materials, in particular for the mesopore region. The choice of the kernel for deriving the PSD for a given nanomaterial should be made based on the a priori information regarding the adsorbent material. Another decisive factor for the choice of a certain kernel is the fitting of the resulting PSD to the experimental isotherm; proper choice of pore geometry leads to better fitting results [14].

In the present work, based on experimental data of high resolution N_2 adsorption isotherm reported by Gor et al. on a CMK-3 sample [1], we present a mixed geometry model, which takes into account the morphological specifics of these nanomaterials. Focused on getting the PSD, which allow to obtain a better characterization of the porous material, we compare different geometrical models, starting with a basic cylindrical pore model followed by a mixed model (cylindrical and slit geometries), which are analyzed by different molecular theories such as the Non-Local Density Functional Theory (NLDFT) [15–17], Quenched Solid Density Functional Theory (QSDFT) [18] and a more detailed molecular model, considering specifically the geometry of the CMK-3 pore, is studied by GCMC. Finally using a virtual solid and the computer "experimental" isotherms, the importance of the pore geometry and its effects on the PSD and isosteric enthalpy of adsorption, are studied.

2. Molecular simulation

2.1. Pore structure and interaction potential models

The GCMC simulation method in the continuum space [19,20], was used to study the adsorption behavior of gases in the CMK-3 material. The first proposed model (the classical model used for CMK-3 materials) considers the interstitial space between the nanorods as a collection of independent cylindrical pores with different sizes. It is assumed that the adsorption occurs only inside of these cylindrical pores.

i) *Cylindrical geometry model (M_Cyl):* For the cylindrical geometry the interactions with the adsorbent are modeled using the Lennard-Jones potential integrated over an infinitely long cylinder [21,22]:

$$u^{sf}(r,R) = \rho_{surf}\varepsilon_{sf}\left(\sigma_{sf}^{12}I_{12} - \sigma_{sf}^{6}I_6\right) \tag{1}$$

where

$$I_{12} = \frac{63\pi^2}{32R^{10}(2-r/R)^{10}}F\left(-\frac{9}{2},-\frac{9}{2};1;(1-r/R)^2\right)$$

$$I_6 = \frac{3\pi^2}{R^4(2-r/R)^4}F\left(-\frac{3}{2},-\frac{3}{2};1;(1-r/R)^2\right)$$

and ρ_{sur} is a two-dimensional density of a carbon cylinder, $F(\alpha,\beta;\gamma;\chi)$ is an hypergeometric function, σ_{sf} and ε_{sf} are the size and energy parameters in the L-J potential between an adsorbed molecule and a carbon atom calculated by the Lorentz-Berthelot rules. The parameter values are shown in Table 1.

ii) *Model of slit and cylindrical pores mixture (M_SlitCyl), with a determined proportion of slit pores* ranging from 0.4 to 2.0 nm and of cylinder pores ranging from 2.0 to 10 nm. This model considers the interstitial space between the nanorods as a collection of independent cylindrical and slit pores (mixture) with different sizes. The cylindrical model was described in point i). For the slit pores, the interaction energy between a fluid particle and a single pore wall at a distance z (measured between the center of the fluid atom and the atoms in the outer layer of the solid) was described as usual by the superposition of two Steele potentials:

$$U_{sf-STEELE}(z) = 2\pi\,\varepsilon_{sf}\rho_C\,\sigma_{sf}^2\Delta \left\{\frac{2}{5}\left(\frac{\sigma_{sf}}{z}\right)^{10} + \left(\frac{\sigma_{sf}}{z}\right)^{4} - \frac{\sigma_{sf}^4}{3\Delta(z+0.61\Delta)^3}\right\} \tag{2}$$

where Δ is the separation between the graphite layers (0.335 nm), ρ_C is the number density of carbon atoms per unit volume of graphite (114 nm^{-3}), and ε_{sf} and σ_{sf} are the solid–fluid L-J parameters.

Furthermore, a model based on experimental data from Solovyovet al. [23] is used in our GCMC simulations. This is a more detailed molecular model, considering specifically the morphology of the CMK-3 pore.

iii) *Model M_CMK3:* The proposed detailed model considers a triangular arrangement of four carbon rods as unit cell, as shown in Figs. 1 and 3. The variable *L* denotes the distance between nanorods; *D* is the nanorod diameter (in our model we fix the value at D = 7), g is the inter-nanorod distance, *d* is the diameter of a cylinder circumscribed between three carbon rods and is defined as the pore size [24]. From Fig. 1 the value of *d=((2L/ 3)-D)* can be obtained.

Each rod is modeled as 5 coaxial graphene sheets as shown in Fig. 2, where R_n and R_{n-1} are the radii of the cylinders number n and n-1, respectively and r_i is the distance from the center line of the carbon rod to an adsorbed molecule. The inter sheet distance ($R_n - R_{n-1}$) was taken equal to that of the graphite, 0.3354 nm.

The interaction potential between an adsorbed fluid molecule and the carbon surface, $u^{sf}(r_i,R_n)$ is described by the sum of the interaction potential of a molecule with each carbon cylinder as shown in the following equations [21,22]:

$$u^{sf}(r_i,R_n) = 4\rho_{surf}\varepsilon_{sf}\sum_{n=1}^{5}\left(\sigma_{sf}^{12}I_{12} - \sigma_{sf}^{6}I_6\right) \tag{3}$$

where

Table 1
Values of Lennard-Jones parameters used in the simulation.

Specie	Parameter	Value
Nitrogen	σ_{ff}	0.3615 nm
	ε_{ff}/k_B	101.4 K
Carbon	σ_{ss}	0.34 nm
	ε_{ss}/k_B	28 K
	ρ_C	38.2 nm^{-2}

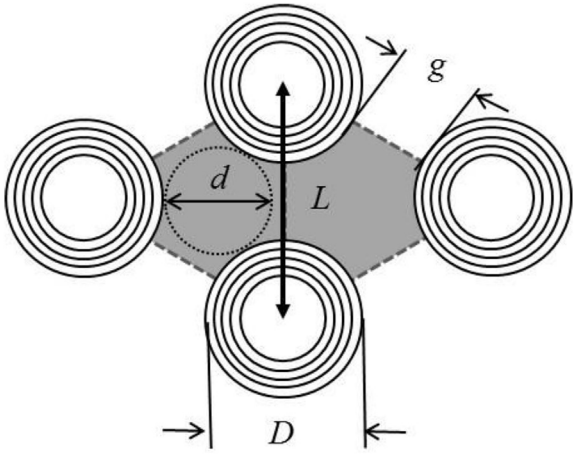

Fig. 1. M_CMK3 model. The unit cell (outlined by dashed line) consists of an arrangement of four carbon rods, where *L* is the unit-cell parameter of the 2-D lattice and d is defined as the pore diameter. The gray area represents the porous space.

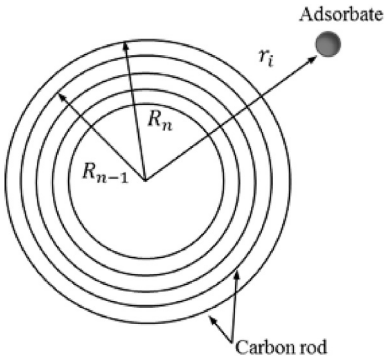

Fig. 2. Schematic illustration of the rod model.

$$I_{12} = \frac{63\pi^2 (R_n/r_i)^{11}}{128 R_n^{10}\{1-(R_n/r_i)^2\}^{10}} F\left(-\frac{9}{2}, -\frac{9}{2}; 1; (R_n/r_i)^2\right)$$

$$I_6 = \frac{3\pi^2 (R_n/r_i)^{5}}{4 R_n^{4}\{1-(R_n/r_i)^2\}^{4}} F\left(-\frac{3}{2}, -\frac{3}{2}; 1; (R_n/r_i)^2\right)$$

and ρ_{surf} is a two-dimensional density of a carbon cylinder, $F(\alpha,\beta;\gamma;\chi)$ is an hypergeometric function, σ_{sf} and ε_{sf} are the size and energy parameters in the L-J potential. The total adsorbate-adsorbent interaction potential for the model (Fig. 3), ϕ_{sf}, is obtained by the sum of the interactions between the fluid molecule and each carbon rod. Finally, in an analogous form as the point ii):

iv) *Model of slit and M_CMK3 pores mixture (M_SlitCMK3), with a determined fraction of slit pores* ranging from 0.4 to 2.0 nm and of M_CMK3 pores ranging from 2.0 to 10 nm. The mixed model considers the porous space as a collection of independent of slit and M_CMK3 pores (mixture), with different sizes.

In all studied cases the intermolecular interaction between the adsorbed molecules, $\varphi_{ff}(r_{ij})$ is modeled using the L-J potential:

$$\varphi_{ff}(r_{ij}) = 4\varepsilon_{ff}\left[\left(\frac{\sigma_{ff}}{r_{ij}}\right)^{12} - \left(\frac{\sigma_{ff}}{r_{ij}}\right)^{6}\right] \quad (4)$$

where, r_{ij} is the intermolecular separation, and ε_{ff} and σ_{ff} are the L-J parameters of fluids [25].

A collection of independent adsorption isotherms for different pore sizes (the local isotherms, θ_L) was obtained through the GCMC method, following the algorithm outlined in Ref. [20], for the geometries described above. Transition probabilities for each Monte Carlo attempt (displacement, adsorption and desorption of molecules), are given by the usual Metropolis rules. The lateral dimensions of the cell for the slit geometry and the longitudinal dimension for the cylindrical geometry were taken as 50 nm, and the periodic boundary conditions were used in those directions. In the M_CMK3 model periodic boundary conditions are imposed in all directions considering the minimum image condition. In general, equilibrium was achieved after 2×10^7 MC attempts, after which mean values were collected over the following 10^7 MC attempts for configurations spaced by 10^3 MC attempts, to ensure statistical independence. Then this collection of isotherms was

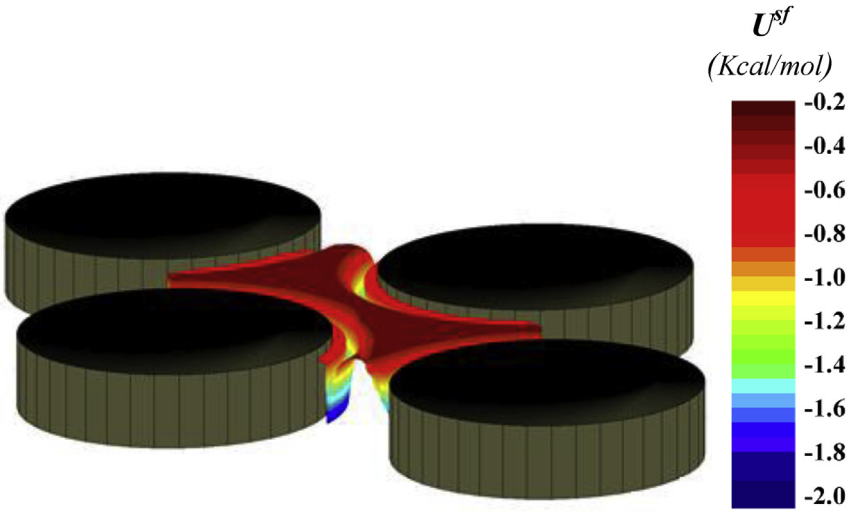

Fig. 3. The total adsorbate-adsorbent interaction potential for the model M_CMK3. The depth of the energy well is shown in a gradient color scale. (A colour version of this figure can be viewed online.)

used in three different ways to fit a given experimental isotherm: M_SlitCyl, M_CMK3 and M_SlitCMK3. The usefulness in a model is measured by its ability to capture the governing physical features of problem [26]. In this paper, we show the usefulness of using these new models (M_CMK3 and M_SlitCMK3) to obtain detailed characterization of these materials.

The accessible pore volume is defined as the space available to the center of an adsorbate molecule where the solid-fluid potential is negative [27]. Thus, the adsorption excess (and therefore the adsorption isotherm) can be calculated.

2.2. Isosteric enthalpy of adsorption

A thermodynamic quantity of interest that can be readily obtained from the GCMC is the "heat of adsorption" [28] (the use of the term isosteric enthalpy of adsorption is recommended by the IUPAC [7]). Additionally, there is difference between absolute and excess heats of adsorption [29]. From a simulation point of view, all of these quantities involve the obtaining of the energetic contribution of adsorption to the isosteric enthalpy of adsorption. Equations (5) and (6) allow us to calculate the heat of adsorption from simulation.

$$q_{st}^{a}(P) = q_{st}(P) - H^{b}(P) = -\left(\frac{\partial U^{a}(P)}{\partial N^{a}(P)}\right)_{T,V^{a}} \tag{5}$$

$$q_{st}^{a}(P) = \left[\frac{U_{ff}^{a}N^{a} - U_{ff}^{a}N^{a}}{N^{a}N^{a} - N^{a}N^{a}}\right] + \left[\frac{U_{sf}^{a}N^{a} - U_{sf}^{a}N^{a}}{N^{a}N^{a} - N^{a}N^{a}}\right] \tag{6}$$

where q_{st}^{a} is the configurational contribution of the adsorbed phase to the isosteric enthalpy of adsorption, H^{b} is the molar enthalpy of the bulk fluid, q_{st} is the absolute isosteric enthalpy of adsorption, U_{ff}^{a} and U_{sf}^{a} are the interaction potentials from the fluid-fluid and the fluid-solid contributions to the total configurational energy of the adsorbed fluid within the pore (simulation), and N^{a} is the total number of particles in the pore with all being a function of pressure, P, at a fixed temperature, T, and pore volume, V^{a}. Equation (6) can be calculated during the course of a GCMC simulation, directly using fluctuation theory [30] where the broken brackets denote the ensemble average obtained from the simulation. Therefore, either Equation (5) or 6 can be used to calculate q_{st}^{a} for a single pore. Equation (5) requires either the fitting of U^{a} as a function of N^{a} for differentiation or a discrete approximation of the differential using changes in U^{a} and N^{a} [31].For nitrogen, the minimum value of the gas–solid potential (Ugs) (corresponding to the maximum differential heat of adsorption at very low adsorbed quantity) is represented in Fig. 4 as a function of the pore size S. The different behavior between the three geometries provides the first indication that the use of just cylindrical kernels is not enough for a reliable characterization. We also show the curve for the triangular geometry (wedge-shaped pore); note the similar behavior with the M_CMK3 model for H/σff <3.5 in this point, the distance between the rods in the M_CMK3 is such that the wedge effect disappears while for the triangular geometry this is present for all pore sizes.

2.3. Calculating the pore-size distribution

Davies and Seaton [32,33] have addressed the problem of calculating the PSD from adsorption data in detail and the most important aspects of the solution procedure are presented in this work.

The experimental adsorption isotherm θ_{Exp} can be approximated as a superposition of independent isotherms corresponding to each pore size (Hj), pressure P and temperature T, called local isotherms, θ_{L}(obtained by GCMC simulation), with a weight corresponding to the pore-size distribution, $f(Hj)$:

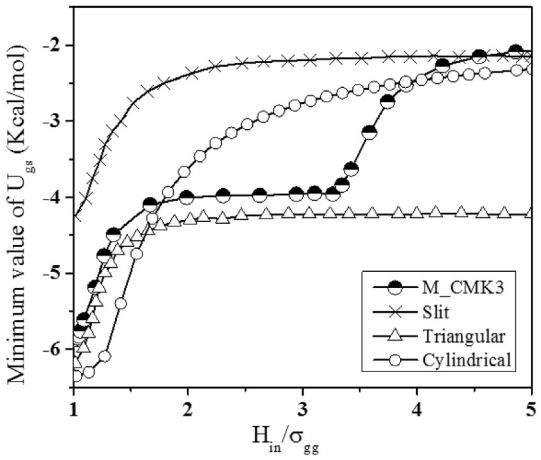

Fig. 4. Minimum value of the gas–solid potential as a function of the pore size. For small pores (<3.5) the Ugs of the M_CMK3 behavior is quite similar to the triangular geometry, whereas as the pore sizes increase this behavior is closer to cylindrical/slit geometries.

$$\theta_{i}^{Exp} \cong \sum_{j=1}^{m} \theta_{L}\left(H_{j}^{*}, P_{i}, T\right) f\left(H_{j}^{*}\right) \delta H_{j}^{*} \tag{7}$$

where m is the number of quadrature intervals used in the analysis and H^{*} is the middle point of each quadrature interval δH^{*}. Equation (7) cannot be directly solved due to the ill-posed and ill-conditioned properties of these equations. However, the detrimental effect of both properties can be minimized by employing regularization [33,34]. The solution of Equation (7) can be obtained by using the non-negative least square method.

3. Results and discussion

In this section, we report molecular simulations of N_2 adsorption at 77 K in the pore models M_SlitCyl, M_CMK3 and M_SlitCMK3. The results are compared with the experimental data of high resolution N_2 adsorption isotherm reported by Gor et al. on a CMK-3 sample [1].

The kernels of selected GCMC adsorption isotherms for the M_Cyl and M_CMK3 models are shown in Fig. 5. The isotherm shapes depend on the pore size and are smooth prior to the capillary condensation steps, which are characteristic of mesopores (>2 nm), and do not exhibit step-wise inflections caused by artificial layering transitions. Although both kernels are qualitatively similar, important differences are observed between them as the pore size decrease. Shown in Fig. 6 are the PSDs from the experimental isotherm derived from the three GCMC kernels: M_SlitCyl, M_CMK3 and M_SlitCMK3, in comparison with that obtained from the QSDFT method with the corresponding geometry (implemented into Quantachrome's data reduction software). Shown in the right side of Fig. 6d–f are the fits of the experimental isotherms obtained by GCMC methods (the M_SlitCMK3 model reports the smallest error by using the same number of parameters).

As a first general observation, the two first PSDs (a-b) have a bimodal distribution from the Monte Carlo and QSDFT method, and all methods are in agreement in the mesopores region (strictly for pores larger than 3 nm), although the PSD obtained by QSDFT is more extended in this region. The M_CMK3 model (Fig. 6b) reports a secondary mesoporous contribution between 2 and 3 nm (the

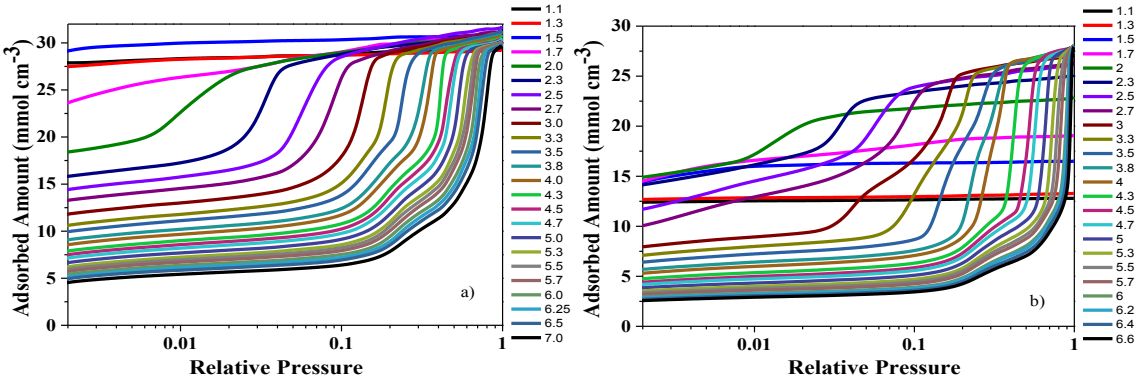

Fig. 5. Kernel of selected simulated adsorption isotherms, for N2 at 77 K using a) M_Cyl model, b) M_CMK3 pore. Shown in the right side the labels of the pores sizes in nm. (A colour version of this figure can be viewed online.)

M_SlitCMK3 method also reports it.) but does not "see" micropores. In the PSD from the M_SlitCMK3 model (Fig. 6c), three peaks can be distinguished, two in the mesopore range and one sharp peak in the micropore region. In the mesoporous region, all the PSDs show a peak around 4.5 nm in agreement with that obtained by X-ray data [1]; furthermore, in the micropores region the best accord

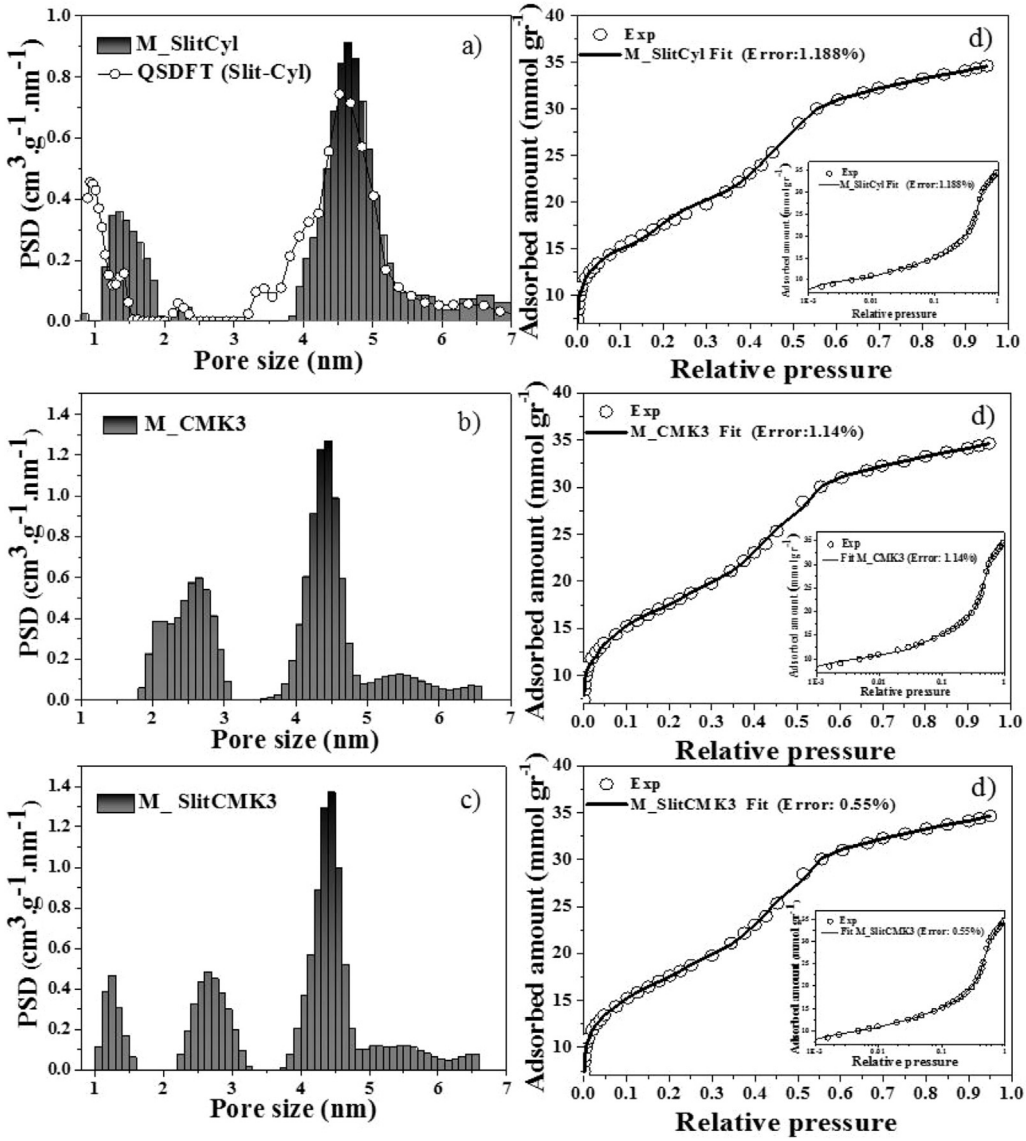

Fig. 6. PSD and experimental isotherm fits obtained from the different GCMC models: (a) M_SlitCyl is compared whit QSDFT methods based on the same geometries (b) M_CMK3 models (c) M_SlitCMK3 mixed model. The respective fitting of the experimental isotherm are shown in (d), (e) and (f). Adsorption isotherms in logarithmic pressure scales are shown in the inset.

(between QSDFT and GCMC) is obtained when the slit geometry is used. Table 2 shows a comparison between the micro/meso pore volumes obtained for the different models. While the change in the total porous volume is relatively small, the proportion of the micropore volume predicted by the M_SlitCMK3 model is significantly lower than the value corresponding to M_SlitCyl. Although these mixed models use the same slit kernel (and in the same interval), the different kernels used in the mesoporous region can modify the fit and the resulting PSD both micro and mesoporous regions.

Zhou et al. [35] reported that CMK-3 includes a small amount of stacked crystalline graphite phase; also Jun et al. [2] reported that the pore walls are constructed by disordered carbon networks similar to activated carbons; and more recently, Onfroy et al. [12], by means of hyperpolarized 129Xe NMR spectroscopy have reported the presence of micropores inside the carbon rods constituting the mesoporous structure of CMK-3 materials. Thus, the origin of the microporosity observed in the PSD can be attributed to small and quite disordered fissures inside the carbon nanorods so that the slit geometry model is more appropriate in this case. On the other hand, the cylindrical geometry model is not the best choice for this kind of adsorbent in the microporous region.

In the mesoporous region, despite the simple geometry and the not precise structure considered according to the known structure of the CMK-3 sample [23], the use of the cylindrical geometry (by using both NLDFT/QSDFT or GCMC) gives good results and is usually assumed for the characterization of CMK-3 materials however, it is possible that we are overlooking important characteristics of this kind of adsorbents that are not "seen" when we use cylindrical pore geometry. In the next paragraphs we discuss this issue in more detail, both from an experimental and theoretical point of view.

By statistical analysis of a TEM image of another CMK-3 sample [3] (different from the Gor et al. sample) and using an appropriate software for analysis of scientific images [36], we obtained the corresponding PSD (histogram in Fig. 7a). The procedure is based on centering a circle between every three rods scanning the complete TEM image and then obtaining the corresponding diameter distribution. It should be noted that this technique presents an inherent limitation due to the TEM does not provide the complete information of the material, although this is presented as a valid complementary tool for solid characterization. We can observe that this kind of nanomaterials can present secondary mesoporosity between 2 and 3 nm, in agreement with the PSD obtained using the M_SlitCMK3 (filled circles in Fig. 7a) and the corresponding experimental isotherm [3]. The fittings of the experimental isotherm using the M_SlitCMK3 and M_SlitCyl models (convolution of the obtained PSD with M_SlitCMK3 and M_SlitCyl kernels isotherms are given in Fig. 7b), are plotted illustrate the good fit with the M_SlitCMK3 (solid line) and M_SlitCyl (dashed line); in this last case the error reported is t is approximately three times bigger than the M_SlitCMK3 error.

In the following paragraphs we discuss the results of a theoretical test using a virtual solid, which shows that assuming a pore geometry model different from the "real" geometry of the sample may lead to different PSD.

Theoretical tests using virtual solids are a useful tool to check models and to explore some properties of porous solids [37,38]. The idea of the test is to generate a virtual solid from a unique (and arbitrary) PSD source and its corresponding pseudo-experimental isotherm. Then, this pseudo-experimental isotherm is fitted by using any given kernel, thus obtaining the resulting PSD.

In this example, using the M_SlitCyl kernel, we calculate the PSD (Fig. 8b) of the pseudo-experimental isotherm obtained through GCMC simulation from a virtual solid (Fig. 8a) composed by a collection of pores (M_CMK3 model) of radius 2.5 and 4.2 nm respectively (Equations (8) and (9)).

$$\theta_{pseudo-\exp erimental}(P_i,T) = f(2,5nm)\theta_{M\_CMK3}(2,5nm,P_i,T)\delta H + f(4,2nm)\theta_{M\_CMK3}(4,2nm,P_i,T)\delta H \quad (8)$$

$$\theta_{pseudo-\exp erimental}(P_i,T) \cong \sum_{j=1}^{m} \theta_{M\_SlitCyl}(H_j,P_i,T) f(H_j)\delta H \quad (9)$$

The PSD obtained (Fig. 8b) (using the same procedure explained in Section 2) is a unimodal distribution, contrary to the real bimodal distribution of the virtual solid, furthermore a bad PSD leads to bad fitting results (Fig. 8d). Therefore, using the M_SlitCyl kernel to obtain the PSD of this virtual M_CMK3 solid it is not a good choice. Based on this particular test we cannot generalize about which kernel to use for the characterization of CMK-3 materials (any characterization method relies on the assumption of a given pore geometry, which must be regarded as an idealization of the real structure of the material), however, the results of this test show that the PSD obtained using a similar kernel can be very different, and therefore it should be carefully interpreted. This is further supported by the results of the isosteric enthalpy of adsorption showed on the right side of Fig. 8. Significant differences between the isosteric enthalpy of adsorption can be appreciated in the inset of Fig. 8c and d) especially in the fluid-solid contribution, due to the heterogeneity inherent in M_CMK3 model.

4. Conclusions

We propose a new Mixed Geometry Model (Slit and M_CMK3) with families of theoretical isotherms obtained through GCMC simulations for the characterization of ordered mesoporous carbon CMK-3 using N_2(77 K) adsorption. The analysis of the adsorption isotherms and predicted PSD, and micro/mesopore volume, reveals that the M_SlitCMK3 model provides a more consistent picture of the sample characteristics than the M_SlitCyl model.

From a simple theoretical test using virtual solids and pseudo-experimental adsorption data, we have shown that assuming a pore geometry model a little different from the "real" geometry of the sample may lead to a very different PSD, even if the effects of accessibility and reliability window are properly ruled out [33,38,39]. These achievements indicate that this is the right way to study this kind of material, where further studies would be needed focused on improving the structural model. It remains for future research studies to compare the relative accuracy of these different approaches to describe and to try to predict isosteric enthalpy of adsorption and to compare them with experimental calorimetric data.

Table 2
Textural properties obtained by the different studied models considering the pore geometries.

Model	Micropore Volume ($cm^3\ g^{-1}$)	Mesopore Volume ($cm^3\ g^{-1}$)	Total Porous Volume ($cm^3\ g^{-1}$)
M_SlitCyl	0.217	0.936	1.153
M_SlitCMK3	0.150	1.106	1.256

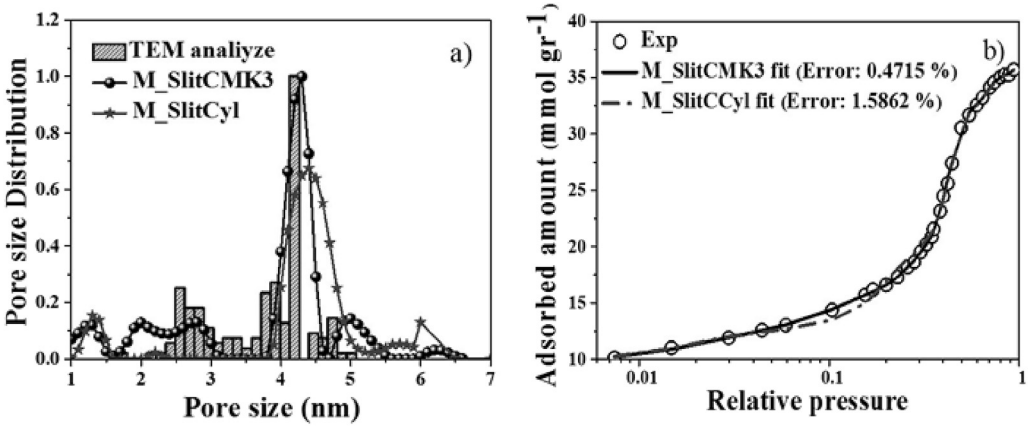

Fig. 7. a) PSDs obtained from the TEM image, M_SlitCyl and M_CMK3 models. b) experimental isotherm fits obtained from the different GCMC models.

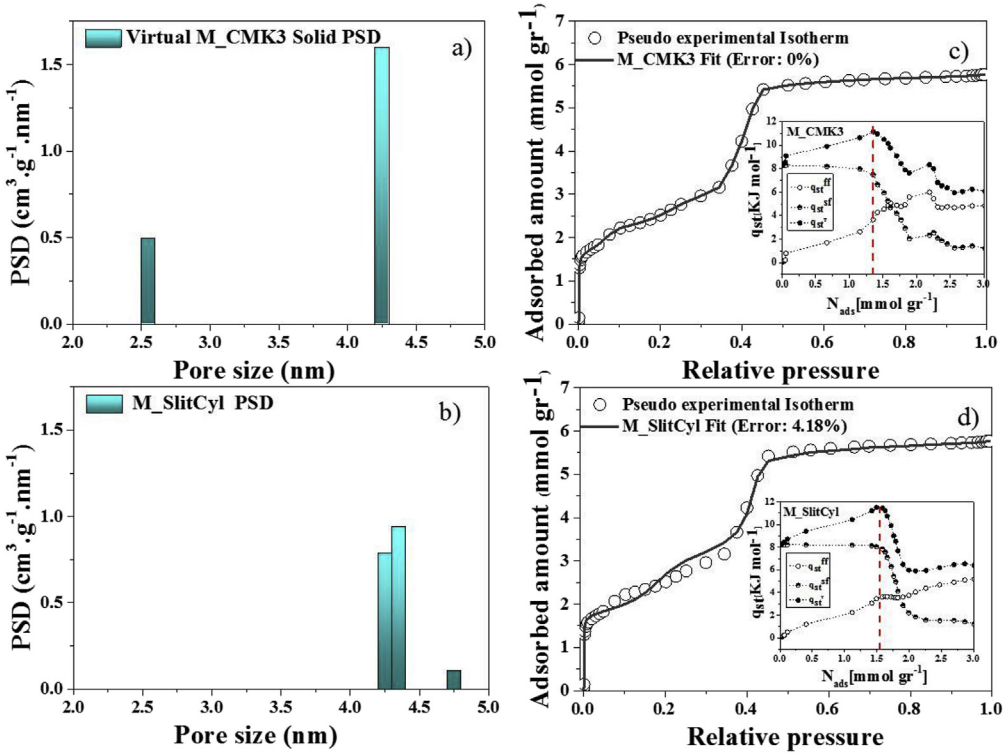

Fig. 8. a) The PSD source that defines the M_CMK3 virtual solid. b) The resulting PSD using the M_SlitCyl kernel. Shown on the right side are shown the corresponding pseudo experimental isotherm c) isosteric enthalpy of adsorption versus surface excess for N_2 adsorption on a virtual M_CMK3 solid and d) the predicted isosteric enthalpy of adsorption using the PSD (M_SlitCyl kernel) from b). The vertical dashed line corresponds to a statistical monolayer. (A colour version of this figure can be viewed online.)

Acknowledgments

This work was financially supported by the UNSL (PROICO: 3-10314), ANPCyT and CONICET. The numerical works were done using the BACO parallel cluster located at the Dpto. de Física - Instituto de Física Aplicada "Giorgio Zgrablich", Universidad Nacional de San Luis- CONICET, San Luis, Argentina. We are also grateful to Professor Octavio Furlong at UNSL for his instructive suggestions.

Appendix A. Supplementary data

Supplementary data related to this article can be found at http://dx.doi.org/10.1016/j.carbon.2017.05.085.

References

[1] G.Y. Gor, M. Thommes, K.A. Cychosz, A.V. Neimark, Quenched solid density functional theory method for characterization of mesoporous carbons by nitrogen adsorption, Carbon N. Y. 50 (2012) 1583–1590, http://dx.doi.org/10.1016/j.carbon.2011.11.037.

[2] S. Jun, S.H. Joo, R. Ryoo, M. Kruk, M. Jaroniec, Z. Liu, T. Ohsuna, O. Terasaki, Synthesis of new, nanoporous carbon with hexagonally ordered mesostructure, J. Am. Chem. Soc. 122 (2000) 10712–10713, http://dx.doi.org/10.1021/ja002261e.

[3] M. Choi, R. Ryoo, Ordered nanoporous polymer-carbon composites, Nat. Mater. 2 (2003) 473–476, http://dx.doi.org/10.1038/nmat923.

[4] S.J. Gregg, K.S.W. Sing, Adsorption, Surface Area and Porosity, second ed., Academic Press, 1982.

[5] F. Rouquerol, J. Rouquerol, K. Sing, Adsorption by Powders and Porous Solids, 1999th ed., Academic Press, 1999.

[6] M. Thommes, Physical adsorption characterization of ordered and amorphous

mesoporous materials, Nanoporous Mater. Sci. Eng. (2004) 317–364.
[7] M. Thommes, K. Kaneko, A.V. Neimark, J.P. Olivier, F. Rodriguez-Reinoso, J. Rouquerol, K.S.W. Sing, Physisorption of gases, with special reference to the evaluation of surface area and pore size distribution (IUPAC Technical Report), Pure Appl. Chem. 0 (2015) 1051–1069, http://dx.doi.org/10.1515/pac-2014-1117.
[8] X. Peng, Z. Qin-Xue, C. Xuan, D. Cao, Acta Phys. -Chim. Sin 27 (2011) 2065–2071.
[9] X. Peng, D. Cao, W. Wang, Heterogeneity characterization of ordered mesoporous carbon adsorbent CMK-1 for methane and hydrogen storage: GCMC simulation and comparison with experiment, J. Phys. Chem. C 112 (2008) 13024–13036, http://dx.doi.org/10.1021/jp8034133.
[10] S.K. Jain, R.J.-M. Pellenq, K.E. Gubbins, X. Peng, Molecular modeling and adsorption properties of ordered silica-templated CMK mesoporous carbons, Langmuir (2017), http://dx.doi.org/10.1021/acs.langmuir.6b04169 acs.langmuir.6b04169.
[11] D. Barrera, M. Dávila, V. Cornette, J.C.A. de Oliveira, R.H. López, K. Sapag, Pore size distribution of ordered nanostructured carbon CMK-3 by means of experimental techniques and Monte Carlo simulations, Microporous Mesoporous Mater. 180 (2013) 71–78, http://dx.doi.org/10.1016/j.micromeso.2013.06.028.
[12] T. Onfroy, F. Guenneau, M.A. Springuel-Huet, A. Gédéon, First evidence of interconnected micro and mesopores in CMK-3 materials, Carbon N. Y. 47 (2009) 2352–2357, http://dx.doi.org/10.1016/j.carbon.2009.04.025.
[13] D.C.S. Azevedo, R.B. Rios, R.H. López, A.E.B. Torres, C.L. Cavalcante, J.P. Toso, G. Zgrablich, Characterization of PSD of activated carbons by using slit and triangular pore geometries, Appl. Surf. Sci. 256 (2010) 5191–5197. http://www.scopus.com/inward/record.url?eid=2-s2.0-77953137392&partnerID=40&md5=041f80c115e91ab0340d23859b646606.
[14] J.P. Toso, V. Cornette, A. Yelpo, J.C.A. De Oliveira, D.C.S. Azevedo, R.H. López, Why the pore geometry model could affect the uniqueness of the PSD in AC characterization, Adsorption (2016), http://dx.doi.org/10.1007/s10450-016-9760-6.
[15] P.I. Ravikovitch, G.L. Haller, A.V. Neimark, Density functional theory model for calculating pore size distributions: pore structure of nanoporous catalysts, Adv. Colloid Interface Sci. 76–77 (1998) 203–226.
[16] A.V. Neimark, P.I. Ravikovitch, Density functional theory of absorption hysteresis and nanopore characterization, Stud. Surf. Sci. Catal. 128 (2000) 51–60.
[17] C.M. Lastoskie, K.E. Gubbins, Characterization of porous materials using density functional theory and molecular simulation, Stud. Surf. Sci. Catal. 128 (2000) 41–50.
[18] A.V. Neimark, Y. Lin, P.I. Ravikovitch, M. Thommes, Quenched solid density functional theory and pore size analysis of micro-mesoporous carbons, Carbon N. Y. 47 (2009) 1617–1628, http://dx.doi.org/10.1016/j.carbon.2009.01.050.
[19] M.P. Allen, D.J. Tildesley, Computer Simulation of Liquids, Oxford University Press, Oxford, 1987.
[20] D. Frenkel, D. Smit, Understanding Molecular Simulation, Academic Press, Sidney, 1991.
[21] W.A. Steele, M.J. Bojan, Simulation studies of sorption in model cylindrical micropores, Adv. Colloid Interface Sci. 76–77 (1998) 153–178, http://dx.doi.org/10.1016/S0001-8686(98)00045-1.
[22] G.J. Tjatjopoulos, D.L. Feke, J.A. Mann Jr., Molecule-micropore interaction potentials, J. Phys. Chem. 92 (1988) 4006–4007.
[23] L.A. Solovyov, A.N. Shmakov, V.I. Zaikovskii, S.H. Joo, R. Ryoo, Detailed structure of the hexagonally packed mesostructured carbon material CMK-3, Carbon N. Y. 40 (2002) 2477–2481.
[24] S.H. Joo, R. Ryoo, M. Kruk, M. Jaroniec, Evidence for general nature of pore interconnectivity in 2-dimensional hexagonal mesoporous silicas prepared using block copolymer templates, J. Phys. Chem. B 106 (2002) 4640–4646, http://dx.doi.org/10.1021/jp013583n.
[25] P.I. Ravikovitch, A. Vishnyakov, R. Russo, A.V. Neimark, Unified approach to pore size characterization of microporous carbonaceous materials from N2, Ar, and CO2 adsorption isotherms, Langmuir 16 (2000) 2311–2320. http://www.scopus.com/inward/record.url?eid=2-s2.0-0033885586&partnerID=40&md5=b19be4dd5d111c368fe49511d13e54af.
[26] D.C.S. Azevedo, R.B. Rios, R.H. López, A.E.B. Torres, C.L. Cavalcante, J.P. Toso, G. Zgrablich, Characterization of PSD of activated carbons by using slit and triangular pore geometries, Appl. Surf. Sci. 256 (2010) 5191–5197. http://www.scopus.com/inward/record.url?eid=2-s2.0-77953137392&partnerID=40&md5=041f80c115e91ab0340d23859b646606.
[27] K. Kaneko, R.F. Cracknell, D. Nicholson, Nitrogen adsorption in slit pores at ambient temperatures: comparison of simulation and experiment, Langmuir 10 (1994) 4606–4609, http://dx.doi.org/10.1021/la00024a036.
[28] T. Vuong, P.A. Monson, Monte Carlo simulation studies of heats of adsorption in heterogeneous solids, Langmuir 12 (1996) 5425–5432, http://dx.doi.org/10.1021/la960325m.
[29] A.L. Myers, P.A. Monson, Adsorption in porous materials at high pressure: theory and experiment, Langmuir 18 (2002) 10261–10273, http://dx.doi.org/10.1021/la026399h.
[30] D. Nicholson, N.G. Parsonage, Computer Simulation and the Statistical Mechanics of Adsorption, Academic Press, London, 1982.
[31] G.R. Birkett, D.D. Do, Correct procedures for the calculation of heats of adsorption for heterogeneous adsorbents from molecular simulation, Langmuir 22 (2006) 9976–9981. http://www.scopus.com/inward/record.url?eid=2-s2.0-33846174316&partnerID=40&md5=a6e9a38a00149e0407157e568ce7ff96.
[32] G.M. Davies, N.A. Seaton, The effect of the choice of pore model on the characterization of the internal structure of microporous carbons using pore size distributions, Carbon N. Y. 36 (1998) 1473–1490. http://www.scopus.com/inward/record.url?eid=2-s2.0-0001704817&partnerID=40&md5=984a8152e3d392d2852a2b04b08191eb.
[33] G.M. Davies, N.A. Seaton, V.S. Vassiliadis, Calculation of pore size distributions of activated carbons from adsorption isotherms, Langmuir 15 (1999) 8235–8245. http://www.scopus.com/inward/record.url?eid=2-s2.0-0033354056&partnerID=40&md5=1c32e35233bca39fe84fae7521916d76.
[34] G.M. Davies, N.A. Seaton, Predicting adsorption equilibrium using molecular simulation, AIChE J. 46 (2000) 1753–1768, http://dx.doi.org/10.1002/aic.690460907.
[35] H. Zhou, S. Zhu, M. Hibino, I. Honma, M. Ichihara, Lithium storage in ordered mesoporous carbon (CMK-3) with high reversible specific energy capacity and good cycling performance, Adv. Mater. 15 (2003) 2107–2111, http://dx.doi.org/10.1002/adma.200306125.
[36] W.S. Rasband, ImageJ, U. S. Natl. Institutes Heal, Bethesda, Maryland, 2016. http://imagej.nih.gov/ij/.
[37] A.D. Lueking, H.-Y. Kim, J. Jagiello, K. Bancroft, J.K. Johnson, M.W. Cole, Tests of pore-size distributions deduced from inversion of simulated and real adsorption data, J. Low. Temp. Phys. 157 (2009) 410–428, http://dx.doi.org/10.1007/s10909-009-9911-1.
[38] J.P. Toso, J.C.A. Oliveira, D.A. Soares Maia, V. Cornette, R.H. López, D.C.S. Azevedo, G. Zgrablich, Effect of the pore geometry in the characterization of the pore size distribution of activated carbons, Adsorption 19 (2013) 601–609, http://dx.doi.org/10.1007/s10450-013-9483-x.
[39] V.Y. Gusev, J.A. O'Brien, N.A. Seaton, A self-consistent method for characterization of activated carbons using supercritical adsorption and grand canonical Monte Carlo simulations, Langmuir 13 (1997) 2815–2821, http://dx.doi.org/10.1021/la960421n.